Published in Semiconductor Science and Technology 21, issue 12, 1743-1746, 2006
which should be used for any reference to this work

A THz quantum cascade detector in a strong perpendicular magnetic field

Giacomo Scalari[1], Marcel Graf[1], Daniel Hofstetter[1], Jérôme Faist[1], Harvey Beere[2] and David Ritchie[2]

[1] Institute of Physics, University of Neuchâtel, CH-2000 Neuchâtel, Switzerland
[2] Cavendish Laboratory, Madingley Rd, Cambridge, UK

Abstract
A 3.6 THz quantum cascade detector is studied under the influence of a strong magnetic field applied perpendicularly to the plane of the layers. Modulation of lifetimes based on elastic intersubband scattering processes is observed, leading to an increase of the responsivity for particular values of the applied magnetic field.

1. Introduction

Since their first demonstration in 2001 [1], THz range quantum cascade lasers (QCLs) have seen a period of rapid progress [2]. With such lasers entering potential applications in spectroscopy and THz imaging [3], there is an increasing demand for small and convenient detectors. Due to their narrow detection linewidth and the photovoltaic operation mode, which both have a positive influence on the noise behaviour, quantum cascade detectors (QCDs) [4, 5] are very promising candidates to fulfil this need. It has been demonstrated recently that QCDs and QWIPs can detect FIR radiation at operating temperatures approaching the critical liquid nitrogen limit [6, 7]. For further improvement of these devices, it is crucial to understand the physical phenomena governing the transport in such structures. As an additional point, the application of an external magnetic field will influence the upper state lifetime in our structures and might therefore improve the detector performance. For this purpose, we investigated a far-IR QCD by magnetospectroscopy. Previous work on this subject is represented by a few theoretical propositions of quantum well detectors based on in-plane magnetic field [8] or on intersubband spin-polarized quantum-well detectors [9], and some work on high-mobility 2DEGs as THz detectors [10].

2. Sample description and experimental apparatus

The structure we have investigated is the THz range quantum well infrared photodetector described in detail in [7] and designed to operate at 3.6 THz. The detector is a QCL-like structure grown in the $Al_{0.15}Ga_{0.85}As/GaAs$ material system on a semi-insulating substrate. The use of a semi-insulating substrate allows the use of the low-loss guiding mechanism based on surface plasmons, which is widely exploited in THz QCLs [1, 11]. The bandstructure is reported in figure 1(*a*): it is obtained using a two-band Kane model and solving the Schrödinger–Poisson problem with a thermal population of the energy levels at $T = 4.2$ K. Non-parabolicity is taken into account via an energy-dependent effective mass, as discussed in [12].

The structure is designed to work under zero bias condition in order to avoid additional noise due to dark current. The operating principle is based on photoexcitation of electrons firstly residing in state $|0\rangle$ into the doublet formed from states $|4\rangle$ and $|5\rangle$ (the calculated energy differences are $E_{50} = 16$ meV and $E_{40} = 13.7$ meV). Once excited in state 4 or 5 the electrons have a certain probability to tunnel into state 3 (ground state of the adjacent well) and then to slide down in the cascade of ground states formed by the chirped superlattice (dashed arrow in figure 1(*a*)). The detector is processed as a mesa structure with a diffraction grating on top (grating pitch 15 μm, duty cycle 50%).

The magnetic field B, applied perpendicularly to the plane of the layers, will split the in-plane energy dispersion into discrete Landau states [13] given by

$$E_{|i,n\rangle} = E_i + \left(n + \frac{1}{2}\right) \frac{\hbar e B}{m^*(E_{|i,n\rangle})}. \qquad (1)$$

Due to the very low value of the GaAs g-factor ($g^*_{\mathrm{GaAs}} = -0.44$), in the following we will neglect the spin degree of freedom. The additional quantization introduced by the magnetic field will decrease the non-radiative processes, enhancing the lifetime $\tau_{5,4\to0}$ and favouring the probability for the electron to tunnel in the adjacent well contributing to the photocurrent. The lifetime of states 4 and 5 will

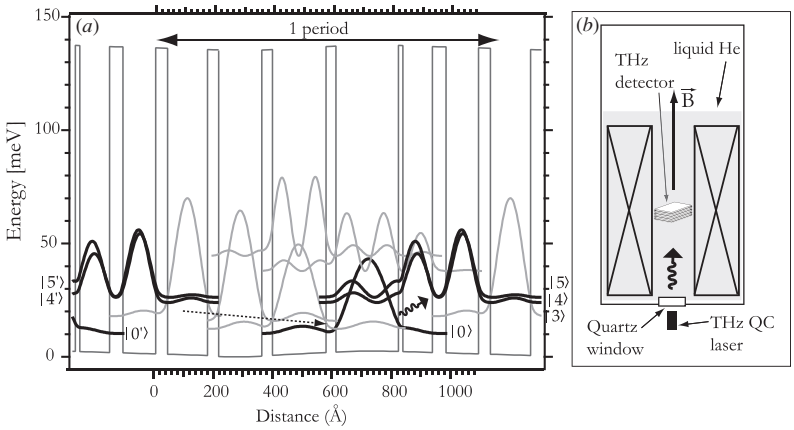

Figure 1. (*a*) Self-consistently calculated conduction band structure for sample A2879 at 4.2 K. One full period, surrounded by adjacent parts of the previous/next period is shown. The layer thicknesses are reported in [7]. The observed transitions take place between the ground state $|0\rangle$ and the states $|4\rangle$ and $|5\rangle$ (bold black lines). The photoexcited electrons are then transported by scattering via the cascade of ground states of the superlattice (dashed arrow). States with energies higher than 50 meV with respect to the bottom of the wells are omitted for clarity. (*b*) Experimental arrangement comprehending a 3.4 THz QC laser placed outside the magnetic field cryostat and shining at constant power through an optical window on the THz QC detector placed in the centre of the superconducting coil and immersed in liquid He.

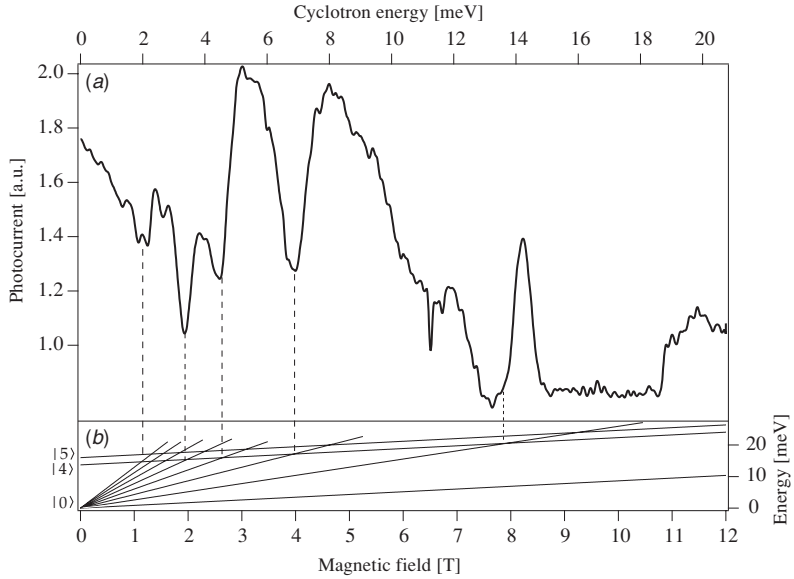

Figure 2. (*a*) Photocurrent signal from sample A2879 as a function of the applied magnetic field, at a temperature $T = 4.2$ K. The vertical dashed lines highlight the correspondence between minima of the photocurrent and elastic resonances that couple the upper and lower levels of the photodetector. (*b*) Landau fan for the three levels $|0\rangle$, $|4\rangle$ and $|45\rangle$ of the photodetector. The energy values are extracted from the bandstructure calculation of figure 1.

be ultimately modulated by the elastic scattering processes [14, 15] which can couple Landau states of different Landau index. Those processes have been already investigated on lasing systems [16–18].

The experimental setup, sketched in figure 1(*b*), is constituted by a THz quantum cascade laser emitting at 87 μm ($h\nu = 14.4$ meV, 3.4 THz, described in [20, 11]) shining at constant power on the detector placed inside the bore of a liquid He cryostat equipped with a superconducting coil [18]. The detector photocurrent is then recorded during the magnetic field sweep. To rule out any possible influence of the stray field of the magnet on the excitation laser, the laser parameters have been monitored controlling their stability throughout the entire magnetic field sweep.

3. Experimental results

The results of a measurement of the detector photocurrent as a function of the applied magnetic field are shown in figure 2(*a*), with the detector temperature kept at $T = 4.2$ K. Panel (b) of the same figure contains a Landau fan of the significant levels of the structure: the energy values are the ones calculated with the Schrödinger–Poisson solver described above and the effect of non-parabolicity is included via the dependence of the effective mass from the cyclotron energy, as visible in formula 1 (see also [19]).

In the region from 0 to 7 T the detector photocurrent shows strong oscillations as a function of the applied magnetic field, with minima located at 1.9 T, 2.6 T and 4 T. In the region

2.8–5.2 T the detector photocurrent (and hence its responsivity) is higher than the value at zero magnetic field. The minima are attributed to elastic resonances between the Landau levels $|4, 0\rangle$ and $|5, 0\rangle$ and the Landau states $|0, j\rangle$ that shorten the lifetime of the excited states increasing the probability of a recapture of the electron in the state $|0\rangle$ and thus producing a loss of responsivity. The minimum at 4 T marks the condition where the energy spacing E_{40} approximately matches twice the cyclotron energy $\hbar\omega_c(4\mathrm{T})$. The deduced value of this energy spacing is 13.7 meV, which matches well the one *calculated* from the bandstructure simulation and is in small disagreement with the one deduced from spectral measurement (14.7 meV [7]). Also the other resonances observed fit with an energy spacing E_{40} of 13.7 meV. The responsivity then drops towards zero and a clean and narrow peak is observed at 8.2 T: this is the cyclotron resonance peak that yields the spectral information about the laser emission frequency. The deduced energy $E_{\mathrm{las}} = \hbar\omega_c(8.2\,\mathrm{T}) = 14.3$ meV matches very well the typical value for the centre of gravity of the mode envelope for a Fabry–Pérot ridge of the kind employed in this experiment.

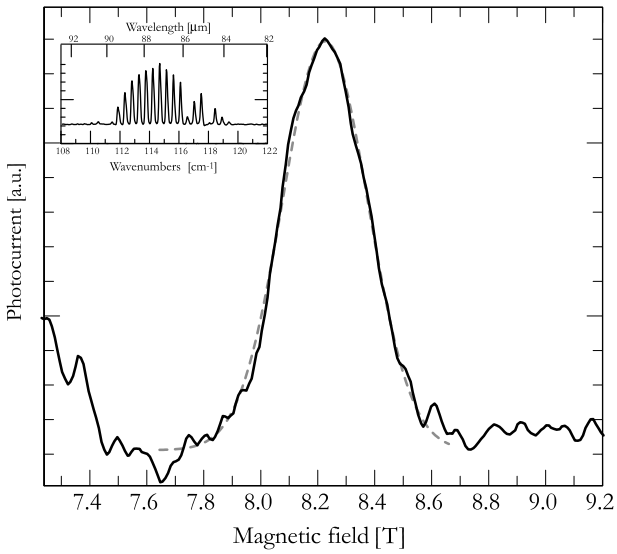

Figure 3. Cyclotron resonance peak (full line) for sample A2879 with an illumination at 14.3 meV. The dashed line is a Gaussian fit that yields a full-width at half max of 0.4 T. Inset: spectral emission of the THz QCL used in the experiment.

4. Discussion

The observed data can be interpreted as follows: the responsivity of the detector will depend on the interplay between the lifetime $\tau_{5,4\to0}$ of one electron in the doublet of states 4, 5 with the total transit time of one electron through a period and thus its contribution to the photocurrent. The magnetic field modulates the lifetime $\tau_{5,4\to0}$ depending on the relative position of the Landau states. When the resonant condition $E_{5,4} - E_0 = \delta n\hbar\omega_c$ (with δn integer representing Landau index change) is satisfied, the lifetime of the upper level is reduced and we expect a diminution of responsivity. When the Landau states are well separated, an increase of the upper state lifetime and, as a consequence, an increase in responsivity is expected. Such effects have been extensively observed on the threshold current of different QC laser structures with energy gaps lying in the THz region [16–18].

At the same time, the localization of carriers induced by an increasing magnetic field will quench the transport, resulting in a poor detector efficiency for high values of applied magnetic fields. The region where the responsivity is higher with respect to the zero field value is the result of the trade-off between the described phenomena: the lifetime $\tau_{5,4\to0}$ is increased and the transport across the structure is not yet heavily affected. The initial decrease of the responsivity in the region 0–1 T is somewhat unexpected: it could be due to resonances between Landau states with high index change but there are no clear signatures to fully support this interpretation.

The discrepancy between the energy difference value of the subbands measured with the FTIR spectrum and the one deduced with the magnetospectroscopy can be ascribed to the depolarization shift. This effect, in a system of two subbands thermally populated with sheet carrier density n_s, blue-shifts the intersubband transition energy according to the following reduced formula [21]:

$$\Delta E_{05} \approx \frac{e^2 n_s}{\epsilon\epsilon_0} S \qquad (2)$$

where S is called the depolarization integral and for an infinite QW of thickness a has the value $S = \frac{5}{9\pi^2}a$ [22]. With the nominal value of the sheet carrier density $n_s = 8.7 \times 10^9$ cm^{-2} we obtain a shift $\Delta E \simeq 0.5$ meV, in good agreement with what observed. Other possible sources of blue shift of the intersubband transition are expected to be less important than the depolarization for our values of energy and electron density [22].

From a Gaussian fit of the cyclotron resonance peak, reported in figure 3 we can deduce a full width at half maximum of 0.4 T that translates into a cyclotron resonance linewidth of 0.69 meV. This value represents the convolution of the cyclotron resonance transition linewidth with the multimode spectrum of the laser. Typical values for cyclotron resonance full widths measured on GaAs/AlGaAs heterostructures [23] are in the 10^{-2}–4×10^{-3} T range. What we observe is then the spectral width of the laser emission that will dominate the detected linewidth: the total width at the base of the peak of 1 meV (8 cm^{-1}) matches well the laser spectrum detected with an FTIR spectrometer and reported in the inset of figure 3. The individual Fabry–Pérot modes of the laser are not resolved because of the resolution on the magnetic field axis. The sweep rate employed gives $\Delta B_{\mathrm{min}} = 0.08$ T, which corresponds to an energy resolution of $\Delta E_{\mathrm{min}} = 0.14$ meV that partially integrates the narrow features.

5. Conclusions

We have investigated a THz range quantum cascade photodetector immersed in a strong magnetic field applied perpendicularly to the plane of the layers. Huge modulations of the photocurrent are observed while sweeping the magnetic field, and are attributed to elastic scattering between the Landau levels of the structure. The observed energy shift of the intersubband transition energy is attributed to many body effects. Further investigation of the system is necessary

in order to clarify the effect of the magnetic field, for example on the thermal activation processes. A spectral characterization of the detector immersed in the magnetic field with a broadband source would also provide insight regarding the many body effects that seem to influence the device spectral response.

Acknowledgments

Financial support from the Swiss National Science Foundation through the project NCCR-Quantum Photonics and the Professorship Program are gratefully acknowledged.

References

[1] Köhler R, Tredicucci A, Beltram F, Beere H, Linfield E, Davies A, Ritchie D, Iotti R and Rossi F 2002 *Nature* **417** 156
[2] Williams B, Kumar S, Hu Q and Reno J 2005 *Opt. Express* **13** 3331
[3] Chamberlin D, Robrish P, Trutna W, Scalari G, Giovannini M, Ajili L and Faist J 2005 *Appl. Opt.* **44** 121
[4] Hofstetter D, Beck M and Faist J 2002 *Appl. Phys. Lett.* **81** 2683
[5] Gendron L, Carras M, Huynh A, Ortiz V, Koeniguer C and Berger V 2004 *Appl. Phys. Lett.* **85** 2824
[6] Luo H, Liu H, Song C and Wasilewski Z 2005 *Appl. Phys. Lett.* **86** 231103
[7] Graf M, Scalari G, Hofstetter D, Faist J, Beere H, Linfield E, Ritchie D and Davies G 2004 *Appl. Phys. Lett.* **84** 475
[8] Huang D and Lyo S 1998 *J. Appl. Phys.* **83** 4531
[9] Savic I, Milanovic V, Vukmirovic N, Jovanovic V, Ikonic Z, Indjin D and Harrison P 2005 *J. Appl. Phys.* **98** 084509
[10] Burke P, Eisenstein J, Pfeiffer L and West K 2002 *Rev. Sci. Instrum.* **73** 130
[11] Ajili L, Scalari G, Faist J, Beere H, Linfield E, Ritchie D and Davies G 2004 *Appl. Phys. Lett.* **85** 3986
[12] Sirtori C, Capasso F, Faist J and Scandolo S 1994 *Phys. Rev.* B **50** 8663
[13] Bastard G 1988 *Wave Mechanics Applied to Semiconductor Heterostructures* (Les Ulis, France: Éditions de Physique)
[14] Raikh M and Shabazyan T 1994 *Phys. Rev.* B **49** 5531
[15] Kempa K, Zhou Y, Engelbrecht J and Bakshi P 2003 *Phys. Rev.* B **68** 085302
[16] Alton J, Barbieri S, Fowler J, Beere H, Muscat J, Linfield E, Ritchie D, Davies G, Köhler R and Tredicucci A 2003 *Phys. Rev.* B **68** 081303
[17] Tamosiunas V, Zobl R, Ulrich J, Unterrainer K, Colombelli R, Gmachl C, West K, Pfeiffer L and Capasso F 2003 *Appl. Phys. Lett.* **83** 3873
[18] Scalari G, Blaser S, Faist J, Beere H, Linfield E, Ritchie D and Davies G 2004 *Phys. Rev. Lett.* **93** 237403
[19] Leuliet A, Vasanelli A, Wade A, Fedorov G, Smirnov D, Bastard G and Sirtori C 2006 *Phys. Rev.* B **73** 085311
[20] Scalari G, Ajili L, Faist J, Beere H, Linfield E, Ritchie D and Davies G 2003 *Appl. Phys. Lett.* **82** 3165
[21] Liu H C and SpringThorpe A 2000 *Phys. Rev.* B **61** 15629
[22] Helm M 2000 *Intersubband Transitions in Quantum Wells: Physics and Device Applications I* vol 62, ed H Liu and F Capasso (New York: Academic) chapter 1, pp 1–99
[23] Hopkins M, Nicholas R, Barnes D, Brummell M, Harris J and Foxon C 1989 *Phys. Rev.* B **39** 13302